

Effect of Electric Field on the Hydrodynamics of Nanoparticles in a Rectangular Fluidized Bed

Mayank Kashyap^{}, Dimitri Gidaspow and Ta-Wei Tsai*

*Department of Chemical and Environmental Engineering, Illinois Institute of Technology,
10 W 33rd St., Perlstein Hall, Chicago, IL 60616*

Abstract

Nanoparticles have unique flow properties that make them useful for numerous applications. Several publications [Zhu et al. (2005), Jung & Gidaspow (2002), Huang et al. (2006)] have recently demonstrated that silica nanoparticles can be fluidized without the formation of bubbles. This property eliminates the major disadvantage of fluidized beds, formation of large bubbles that cause gas bypassing and hence poor reaction.

The effect of electric field on 10 nm silica particles was studied in a specially designed rectangular fluidized bed having an internal cross section of 4.5 in. x 5.5 in., with electrodes attached to two parallel walls. Experiments were conducted using various combinations of superficial gas velocities and electric field strengths.

The bed height decreased drastically on the application of electric field. The decrease was almost linear at 0.70 kV/cm. It was non-linear and larger at 1.05 kV/cm and 1.40 kV/cm. These observations were reverse of those obtained earlier [Wittmann & Ademoyega (1987)] with 177-210 micrometer silica gel particles. The average size of the agglomerates was calculated at various electric fields, using the Richardson-Zaki equation. The size increased from 204 μm to 396 μm when the electric field was increased from 0 kV/cm to 1.40 kV/cm.

Particle density profiles were also determined as a function of solids volume fraction and bed height at different electric fields. These data allowed the computation of granular temperatures using a one dimensional particle momentum balance with the ideal equation of state [Driscoll & Gidaspow (2006)]. This balance is similar to a barometric formula for gases. The granular temperature decreased with the increase in electric field.

* Correspondence concerning this article should be addressed to Mayank Kashyap at kashmay@iit.edu

Introduction

Nanoparticles have unique flow properties that make them useful for numerous applications. Several publications [Zhu et al. (2005), Jung & Gidaspow (2002), Huang et al. (2006)] have recently demonstrated that silica nanoparticles can be fluidized without the formation of bubbles. This property eliminates the major disadvantage of fluidized beds, formation of large bubbles that cause gas bypassing and hence poor reaction.

Theoretical Background- Granular Temperature in a Rectangular Bed

The one dimensional solids momentum balance [Gidaspow,1994] assuming negligible acceleration, negligible wall friction, and zero average solids velocity is given by:

$$\frac{d\sigma_s}{dX} + g\varepsilon_s(\rho_s - \rho_g) = \beta_B v_g \quad (1)$$

In this equation the drag force balances the solids pressure and the buoyant force. Solids pressure can be expressed by the following relationship from the kinetic theory of granular flow [Gidaspow, 1994]:

$$\sigma_s = \rho_s \varepsilon_s \theta \quad (2)$$

Assuming constant granular temperature, the solution of the first order differential equation formed by the above two equations, is found as follows [Driscoll & Gidaspow (2006)]:

$$\text{Log} \left[\frac{\varepsilon_{s0} - \varepsilon_{s,avg.}}{\varepsilon_s - \varepsilon_{s,avg.}} \right] = \frac{g}{\theta} X \quad (3)$$

By using this relationship, the granular temperature may be calculated by utilizing experimental data containing the solids volume fraction as a function of fluidized bed height.

Experimental Description

A series of experiments were conducted to understand the effect of electric field on the hydrodynamics of nanoparticles in a rectangular bed. The fluidized bed used for the

experiments was constructed of 0.25" glass plate with the inside dimensions as 5.5" depth by 4.5" width by 48.25" height. At the base of the rectangular bed was a fine 304 L stainless steel wire support grid (165x1400 mesh) to support the particle bed. A 4.75" high gas distributor was located directly below the support grid. The distributor was filled with plastic packings to allow proper distribution of air. Two 24.5" high copper sheets, acting as the two electrodes with opposite polarities, were attached to parallel walls in the rectangular bed. Each electrode was connected to one of the two High Voltage D.C. Power Supplies (FC8P15 and FC8N15) produced by Glassman High Voltage Incorporated. The D.C. Power Supplies were capable of producing up to 8 kV of D.C. voltage with opposite polarities, thus producing a maximum of 16 kV when connected to the electrodes. One end from each voltage supply was grounded. Compressed air was conditioned prior to entering the fluidized bed. First, the air was heated by an electric heater in the form of a coil wound around the pipe. The air was then flown through a silica gel bed to remove water from the air stream, and it was then regulated with a manual valve before directing through a rotameter. Air from the fluidized bed was discharged to the atmosphere. A diagram of the rectangular fluidized bed is shown in Figure 1.

The fluidized bed was charged with Tullanox 500, which is a fumed silica having a typical particle size of 10 nanometers. Tullanox particles tend to form agglomerates that are typically of the order of 200 micrometers. The tests to measure the bed expansion at various superficial gas velocities, and to see the effect of electric field on the height of the fluidized bed upon the application of electric field were conducted by adding a small amount of Tullanox to the fluidized bed, recording the mass of material, volume of the fluidized bed, and the voltage generated. The bed was fluidized at five different superficial gas velocities. The electric field was then applied independently having the strengths of 0.70 kV/cm, 1.05 kV/cm and 1.40 kV/cm. The final height of the bed was noted to measure the bed expansion upon the application of electric field. Similar experiments were conducted to see the effect of electric field on the fluidized bed height with time upon the application of electric field.

The solids volume fraction in the fluidized bed was measured by recording the voltage generated from a photovoltaic sensor when a light source was passed through the fluidized bed [Driscoll, 2006]. The rectangular fluidized bed was equipped with a high intensity source (a Fiber lite- A 3200 with a 200 watt bulb). The light source provided a constant color, uniform light source with intensity control. The voltage generation cell was a high-speed borosilicate

detector (Edmunds Optics model NT55-338 15 mm²). The voltage generated by the detector is inversely proportion to the solids volume fraction of the fluidized bed. The voltage signal was collected using a National Instruments data collection system. The voltage signal was sent to a NI SCC-AI 05-2 channel 100 mV analog input module. This module resides in a NI SCC-6221 M Series Multifunction DAQ card in the PC. The experimental data were collected and saved into an Excel spreadsheet utilizing Labview software.

The calibration method was also conducted by adding a small amount of Tullanox to the fluidized bed, recording the mass of material, volume of the fluidized bed, and the voltage generated. For each volume, an average of the several measurements at a given volume was taken at the representative voltage corresponding to the solids volume fraction. The bed was expanded to several different volumes by injecting compressed air into the bed at various superficial gas velocities and under the influence of various electric fields. The data were recorded at each set of conditions and a calibration curve was developed. The calibration curve is presented in Figure 14. The calibration procedure established a representative voltage for each solids volume fraction.

Results and Discussion

Bed expansion

The silica nanoparticle bed expanded linearly with the increase in the superficial gas velocity, at no electric field. Figure 2 compares the bed expansion observed by Zhu et al. (2005), Vasishta (2004) and Kalra (2005). Zhu et al. (2005) observed almost a linear expansion of the bed with the increase in superficial gas velocity. Vasishta (2004) and Kalra (2005) independently observed an abrupt increase in the bed expansion at gas velocities in the range of 1 cm/s to 1.5 cm/s. Figure 3 shows that the expansion in the fluidized bed at increasing superficial gas velocities was linear at 0 kV/cm and 0.70 kV/cm. The expansion was shown by a combination of two linear curves having lower order of magnitude at 1.05 kV/cm and 1.40 kV/cm. Figure 4 shows the effect of electric field on the fluidized bed height, at various superficial gas velocities. The observations were reverse of those obtained by Wittmann & Ademoyega (1987) with 177-210 micrometer silica gel particles, who observed an increase in the bed height on the application of electric field. The decrease in the bed height of charged

silica nanoparticles on the application of electric field is due to the downward acting electric force.

Bed height versus time

The height of the bed decreased drastically on the application of electric field. Figures 5 to 9 show that the decrease was non-linear, larger and faster at 1.40 kV/cm as compared to that at 0.70 kV/cm. The decrease in the bed height was larger and faster at 3.69 cm/s gas superficial velocity as compared to that at 0.99 cm/s gas superficial velocity.

Voltage output versus height in fluidized bed

The calibration curve showed a particle density gradient within the fluidized bed on the application of electric field. Figures 10 to 13 show that the voltage generated by the photovoltaic sensor first increased, then decreased, and again increased as the sensor was moved up from the bottom of the bed. The voltage was low at the bottom of the bed due to the effect of gravity. It increased on moving up due to the presence of dilute region of particles. The voltage decreased just below the interface. This was due to the high order of cancellation of velocities of the particles in the upward and downward directions, in the presence of electric field. The voltage again increased at the interface. This trend was different from that seen by Vasishta (2004), who saw a continuous increase in the generated voltage from the bottom of the bed without the application of electric field.

Calibration curve

Figure 14 shows that the solids volume fraction was inversely related to the voltage generated by the sensor within the fluidized bed. At no electric field, the curve had a similar trend as those obtained by Driscoll & Gidaspow (2006) and Vasishta (2004).

Height in fluidized bed versus Solids Volume Fraction

Figures 15 to 18 show the variation of solids volume fractions with height within the fluidized bed, at various superficial gas velocities and electric fields. The solids volume fraction was the highest at the bottom of the bed. The solids volume fraction first decreased, then increased and again decreased on moving up in the bed. This result was in congruence with the

calibration curve explained above. Solids volume fraction was higher at 0.99 cm/s & 1.40 kV/cm than at 3.69 cm/s & 0 kV/cm.

Terminal velocity & average size of fluidized agglomerates

Figure 19 shows that $U_g^{1/n}$ versus H_0/H_1 (Zhu et al., 2005), for Richardson-Zaki exponent n equal to 5, at various electric fields are straight lines. The slopes of the lines increased as the electric field was increased from 0 kV/cm to 1.40 kV/cm. The average size of the particles was increased from 204 μm to 396 μm when the electric field was increased from 0 kV/cm to 1.40 kV/cm. This was due to the fact that electric field caused the particles to stick together while moving towards the electrodes. The terminal velocity of the agglomerates increased from 5.9 cm/s to 22 cm/s in the same range of electric field. This was due to the increase in size of the agglomerates. Table 1 compares the average size of agglomerates for different types of nanoparticles presented here, published by Zhu et al. (2005), Vasishta (2004) and Kalra (2005). The calculated terminal velocities and the average agglomerate sizes were comparable with those obtained by Zhu et al. (2005).

Granular temperature

Slopes from the plots of $\text{Log}\left(\frac{\varepsilon_{s0} - \varepsilon_{s,avg.}}{\varepsilon_s - \varepsilon_{s,avg.}}\right)$ versus X were used to compute the granular

temperatures at various superficial gas velocities and electric fields. Figures 20 and 21 show that the granular temperature decreased with the increase in electric field. It decreased with the decrease in superficial gas velocities. Table 2 summarizes the effect of superficial gas velocity and electric field on granular temperature.

Conclusions

Fluidization of fumed silica nanoparticles in a batch system is strongly affected by the application of an electric field of the order of 1 kV/cm. Both the bed expansion and the granular temperature decrease drastically upon the application of the electric field. For example, the granular temperature decreased from 0.93 m^2/s^2 to 0.3 m^2/s^2 with an electric field of 1.4 kV/cm, at a superficial gas velocity of 3.7 cm/s. The effective agglomerate size increased from 204 μm

to 396 μm upon the application of the electric field of 1.4 kV/cm. This mechanism may provide a means of controlling the fluidized bed and of reducing elutriation from the fluidized bed.

Acknowledgement

We thank the National Science Foundation (NSF) for partial financial support through Grant # DMI 0210400, and the co-principal investigators of this NSF project, Prof. Hamid Arastoopour of Illinois Institute of Technology and Prof. Robert Pfeffer of New Jersey Institute of Technology.

Notation

d_a = average size of fluidized agglomerates, μm

g = gravitation constant, cm/s^2

H_0 = initial bed height, cm

H_1 = height of fluidized bed without electric field, cm

H_2 = height of fluidized bed upon application of electric field, cm

n = exponent in the Richardson-Zaki equation, dimensionless

U_g = superficial gas velocity, cm/s

U_{pt} = terminal velocity for a single agglomerate, cm/s

v_i = velocity of "i" phase, cm/s

X = distance from the top of the initial bed, cm

Greek letters

β_B = gas-solid drag coefficient for Model B, $\text{g/cm}^3\text{-s}$

ρ_s = particle density, g/cm^3

ρ_g = density on gas, g/cm^3

ϵ_s = solids volume fraction, dimensionless

ϵ_0 = solids volume fraction at $X = 0$, dimensionless

$\epsilon_{s,avg.}$ = average solids volume fraction, dimensionless

θ = granular temperature, m^2/s^2

σ_s = solids stress, dyn/cm^2

References

- R.B. Bird, W.E. Stewart & E.N. Lightfoot. Transport Phenomena, 2nd Edition, John Wiley and Sons, New York, 2002
- Michael Driscoll. A Study of the Fluidization of FCC and Nanoparticles in a Rectangular Bed and a Riser. Ph.D. Thesis, Illinois Institute of Technology, Chicago, In Progress, 2006
- Michael Driscoll & Dimitri Gidaspow. Wave Propagation and Granular Temperature in Fluidized Beds of Nano and FCC Particles. AIChE Annual Meeting, San Francisco, 2006
- Dimitri Gidaspow. Multiphase Flow and Fluidization: Continuum and Kinetic Theory Descriptions, Academic Press, New York, 1994
- Cang Huang, Yao Wang & Fei Wei, 2006. Multi-Stage Agglomerate Structure and Solids Mixing Behavior of Nano-Particle in Fluidized Bed. 5th World Congress on Particle Technology, Orlando, 2006
- Jonghwun Jung & Dimitri Gidaspow. Fluidization of Nano-Size Particles. Journal of Nanoparticle Research 4: 483-497, 2002
- Jailesh Kalra. Fluidization of Silica Nano-Size Particles in Circulating and Two Dimensional Fluidized Beds. Masters Thesis, Illinois Institute of Technology, Chicago, 2005
- Viju Vasishta. Hydrodynamics of Fluidization and Settling of Silica Nanoparticles. Masters Thesis, Illinois Institute of Technology, Chicago, 2004
- Charles V. Wittmann & Benjamin O. Ademoyega. Hydrodynamic Changes and Chemical Reaction in a Transparent Two-Dimensional Cross-Flow Electrofluidized Bed. 1. Experimental Results. Ind. Eng. Chem. Res. 1987, 26, 1586-1593
- Chao Zhu, Qun Yu, Rajesh N. Dave & Robert Pfeffer, 2005. Gas Fluidization of Nanoparticle Agglomerates. AIChE Journal. 51: 426-439

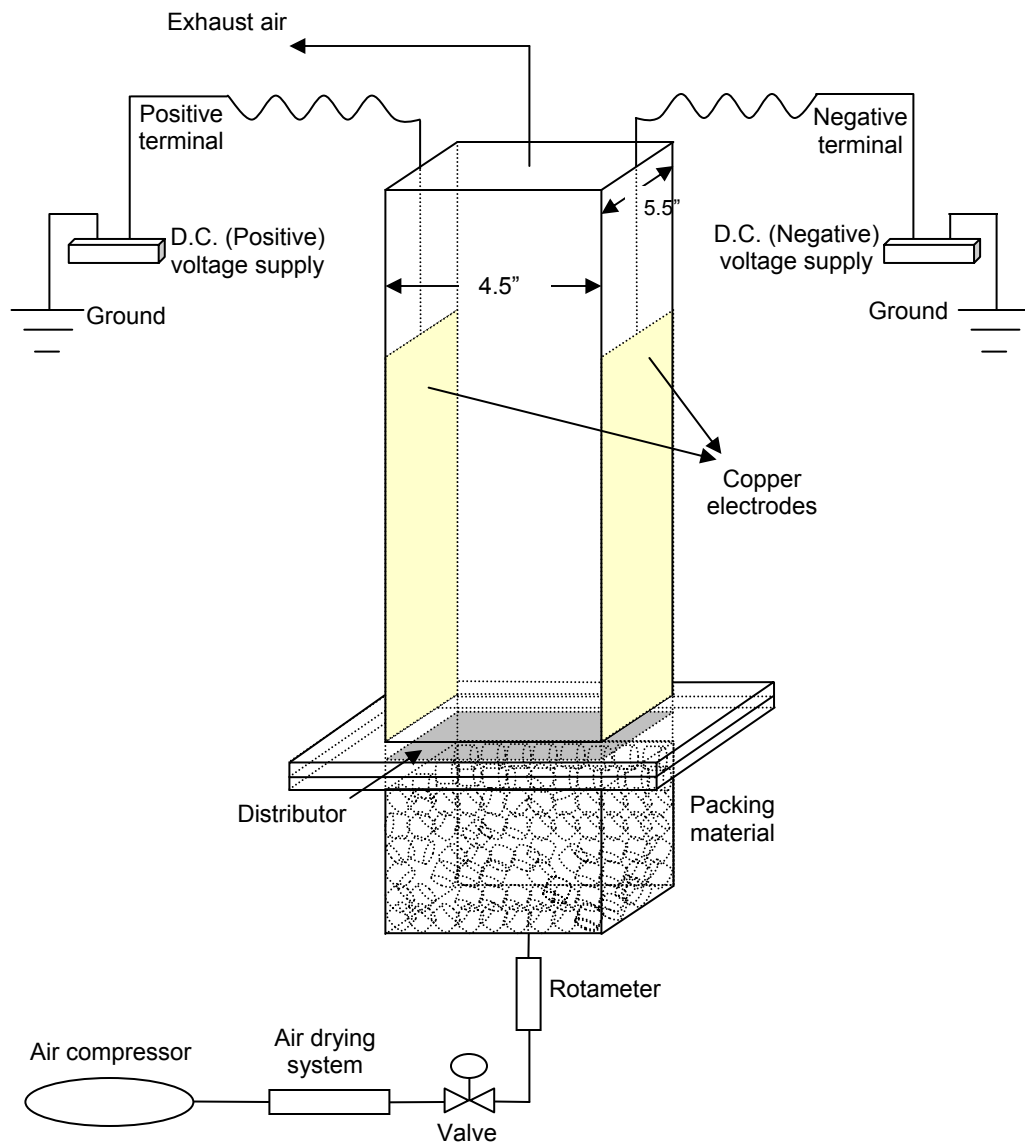


Figure 1. Experimental setup of the rectangular fluidized bed, with electrodes attached on two parallel walls.

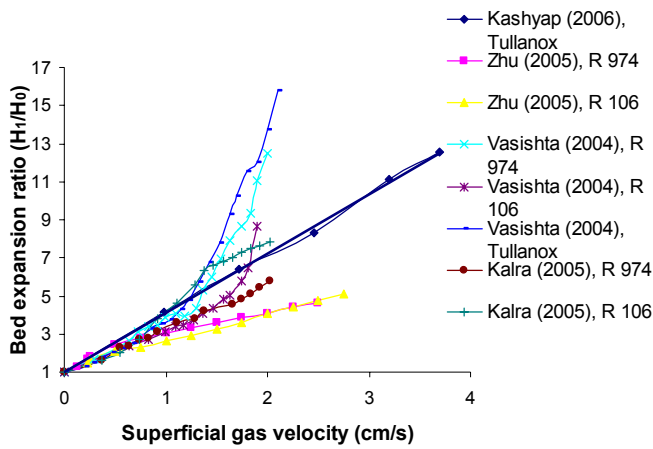


Figure 2. Comparison of bed expansion ratios without electric field, at various superficial gas velocities.

Straight line is a linear regression result, given by the equation $y = 3.1191x + 0.9879$, with an R-sq. value of 99.8%.

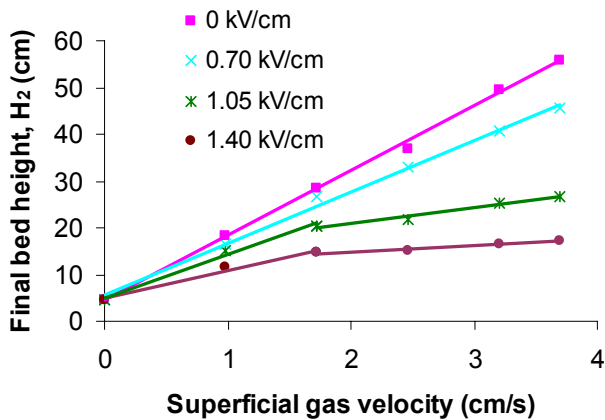


Figure 3. Fluidized bed height upon the application of electric field, at various superficial gas velocities.

Straight lines are represented by the following equations: $y = 13.865x + 4.391$ at 0 kV/cm; $y =$

$12.274x + 5.0507$ at 0.35 kV/cm; $y = 11.073x + 5.5617$ at 0.70 kV/cm; $y = 9.3022x + 4.9341$ at 1.05 kV/cm up to superficial gas velocity of 1.72 cm/s; $y = 3.4375x + 13.97$ at 1.05 kV/cm and higher superficial gas velocities; $y = 5.9576x + 4.7797$ at 1.40 kV/cm up to superficial gas velocity of 1.72 cm/s; $y = 1.3329x + 12.182$ at 1.40 kV/cm and higher superficial gas velocities.

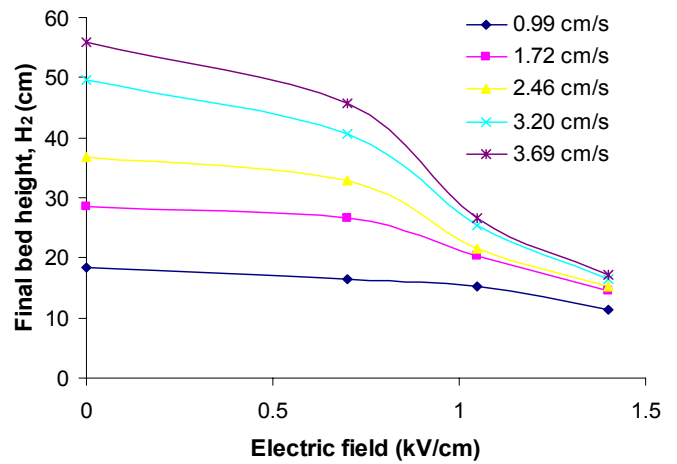


Figure 4. Effect of electric field on the fluidized bed height, at various superficial gas velocities.

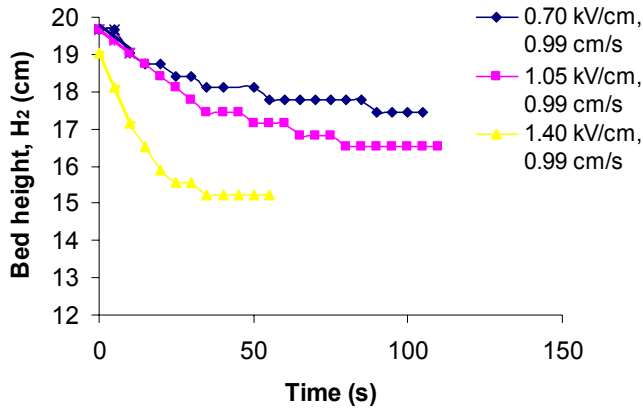


Figure 5. Effect of electric field on the fluidized bed height with time upon the application of electric field, at a superficial gas velocity of 0.99 cm/s.

The initial slope lines are represented by the following equations: $y = -0.0635x + 19.791$ at 0.70 kV/cm; $y = -0.0635x + 19.685$ at 1.05 kV/cm; $y = -0.1905x + 19.05$ at 1.40 kV/cm.

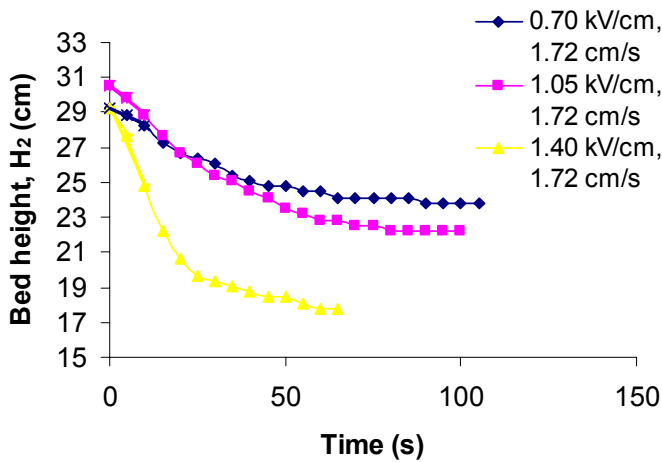


Figure 6. Effect of electric field on the fluidized bed height with time upon the application of electric field, at a superficial gas velocity of 1.72 cm/s.

The initial slope lines are represented by the following equations: $y = -0.0952x + 29.263$ at 0.70 kV/cm; $y = -0.1588x + 30.533$ at 1.05 kV/cm; $y = -0.4445x + 29.422$ at 1.40 kV/cm.

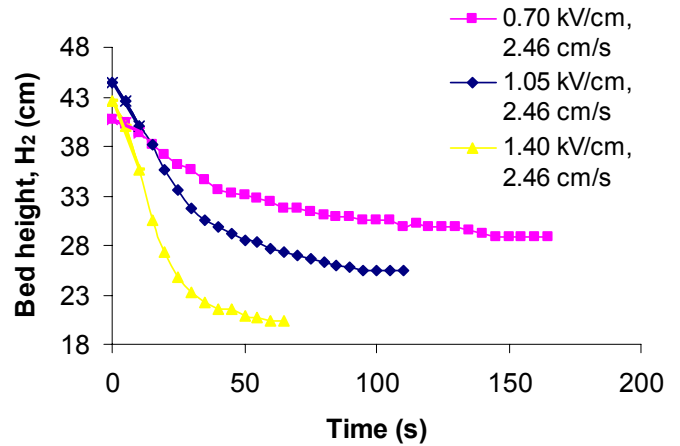


Figure 7. Effect of electric field on the fluidized bed height with time upon the application of electric field, at a superficial gas velocity of 2.46 cm/s.

The initial slope lines are represented by the following equations: $y = -0.127x + 40.746$ at 0.70 kV/cm; $y = -0.4445x + 44.556$ at 1.05 kV/cm; $y = -0.6985x + 42.863$ at 1.40 kV/cm.

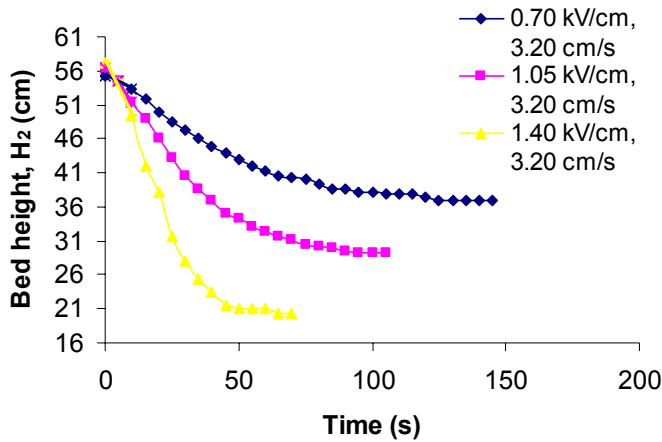


Figure 8. Effect of electric field on the fluidized bed height with time upon the application of electric field, at a superficial gas velocity of 3.20 cm/s.

The initial slope lines are represented by the following equations: $y = -0.1905x + 55.351$ at 0.70 kV/cm; $y = -0.508x + 56.727$ at 1.05 kV/cm; $y = -0.762x + 57.573$ at 1.40 kV/cm.

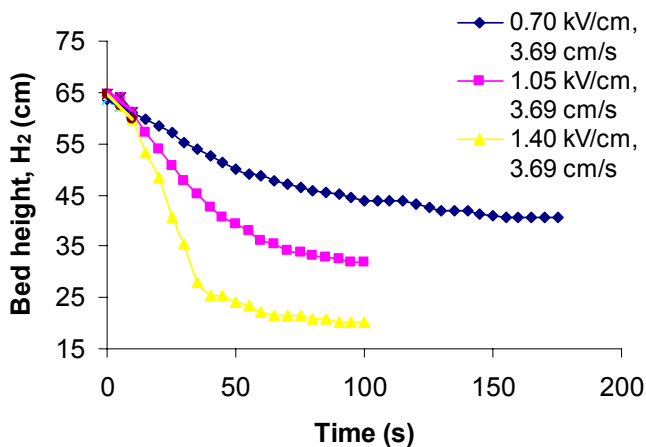


Figure 9. Effect of electric field on the fluidized bed height with time upon the

application of electric field, at a superficial gas velocity of 3.69 cm/s.

The initial slope lines are represented by the following equations: $y = -0.254x + 63.5$ at 0.70 kV/cm; $y = -0.381x + 65.193$ at 1.05 kV/cm; $y = -0.508x + 64.77$ at 1.40 kV/cm.

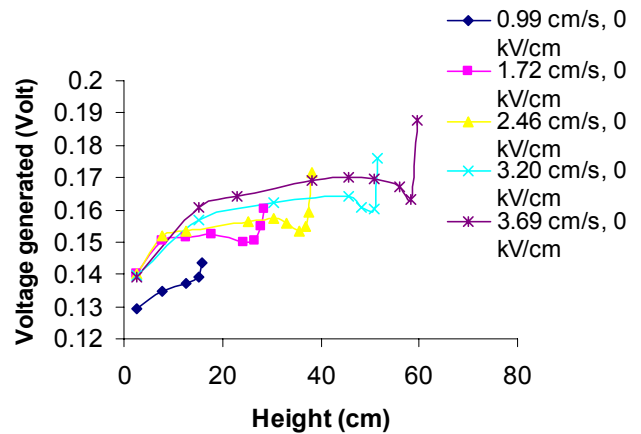


Figure 10. Voltage generated from a photovoltaic sensor versus height within the fluidized bed without electric field, at various superficial gas velocities.

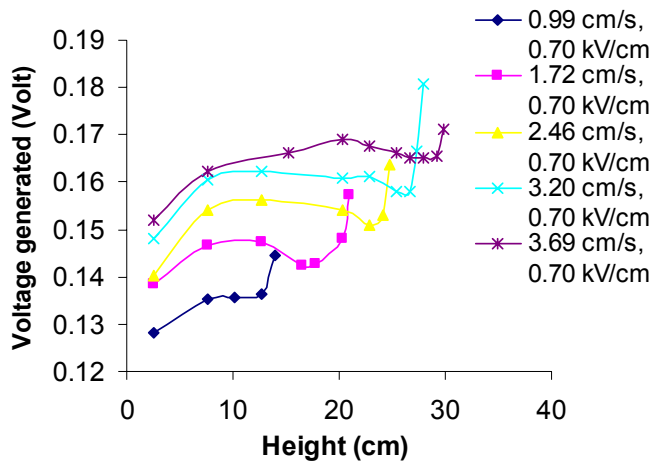


Figure 11. Voltage generated from a photovoltaic sensor versus height within the fluidized bed with an electric field of 0.70 kV/cm, at various superficial gas velocities.

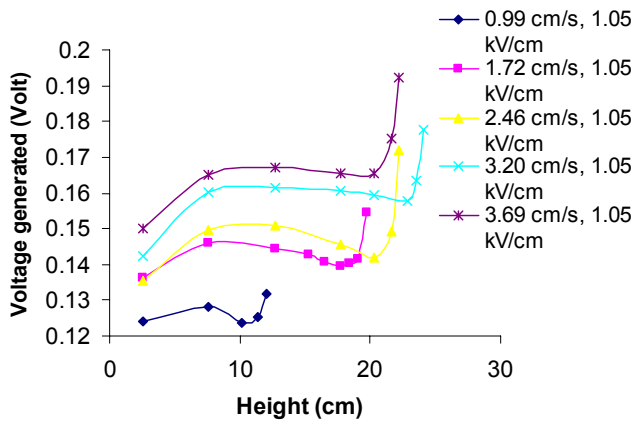


Figure 12. Voltage generated from a photovoltaic sensor versus height within the fluidized bed with an electric field of 1.05 kV/cm, at various superficial gas velocities.

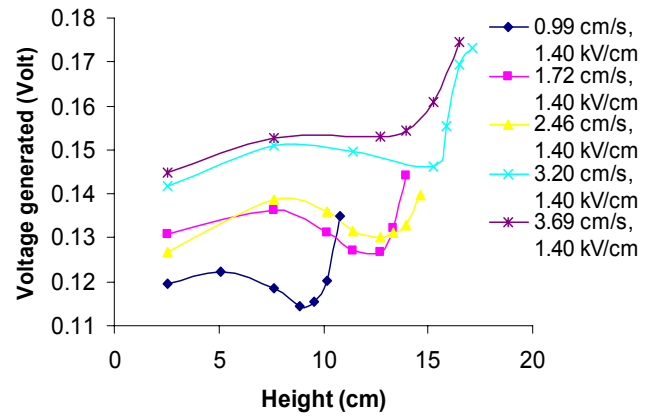


Figure 13. Voltage generated from a photovoltaic sensor versus height within the fluidized bed with an electric field of 1.40 kV/cm, at various superficial gas velocities.

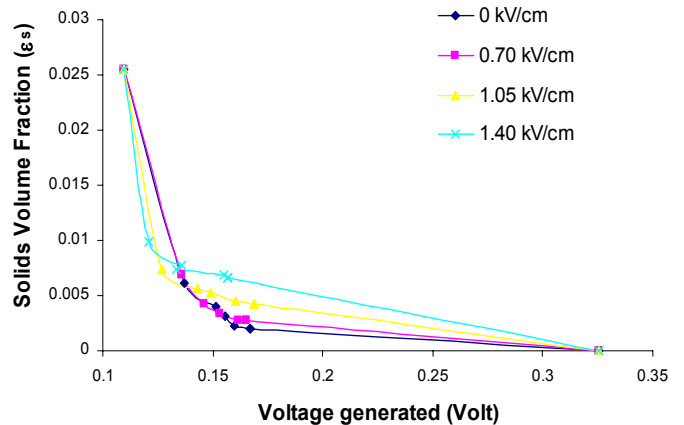


Figure 14. Calibration curve for rectangular fluidized bed at various electric field strengths.

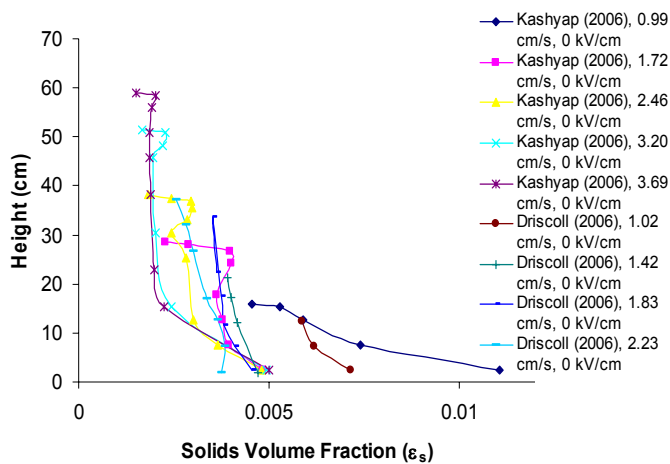


Figure 15. Solids Volume Fraction versus height in the fluidized bed without electric field, at various superficial gas velocities.

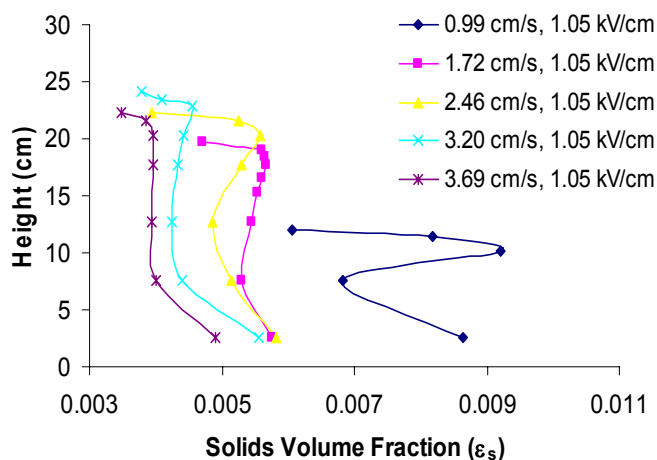


Figure 17. Solids Volume Fraction versus height in the fluidized bed with an electric field of 1.05 kV/cm, at various superficial gas velocities.

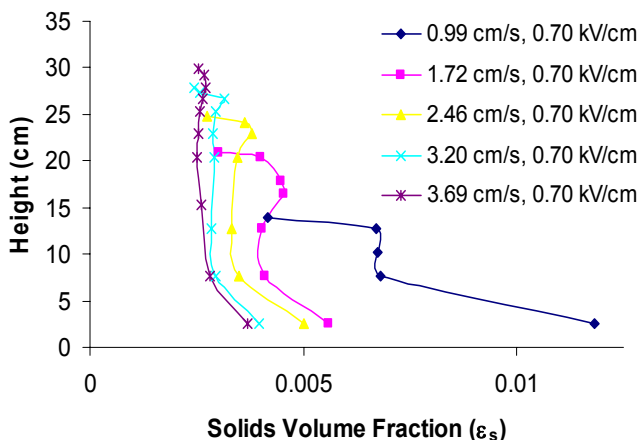


Figure 16. Solids Volume Fraction versus height in the fluidized bed with an electric field of 0.70 kV/cm, at various superficial gas velocities.

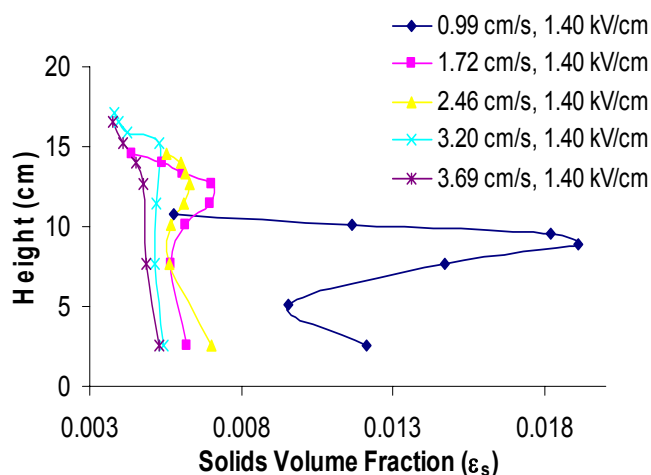


Figure 18. Solids Volume Fraction versus height in the fluidized bed with an electric field of 1.40 kV/cm, at various superficial gas velocities.

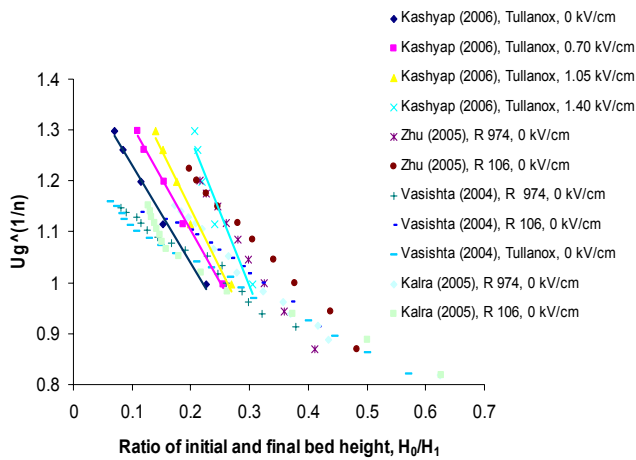


Figure 19. Richardson-Zaki plot for the determination of average size of fluidized agglomerates, at various electric field strengths.

Straight lines are linear regression results, for a Richardson-Zaki exponent n equal to 5.

Table 1. Comparison of agglomerate size, using Richardson-Zaki exponent n equal to 5, at various electric field strengths.

	Particles	Electric Field (kV/cm)	U_{pt} (cm/s)	d_a (μm)
Kashyap (2006)	Tullanox	0	5.86	203.92
Kashyap (2006)	Tullanox	0.7	7.98	237.92
Kashyap (2006)	Tullanox	1.05	10.88	277.86

Kashyap (2006)	Tullanox	1.4	22.05	395.57
Zhu (2005)	R 974	0	5.09	211
Zhu (2005)	R 106	0	6.21	201
Zhu (2005)	R 972	0	6.04	195
Vasishta (2004)	R 974	0	2.50	133.11
Vasishta (2004)	R 106	0	3.03	146.61
Vasishta (2004)	Tullanox	0	2.21	125.11
Kalra (2005)	R 974	0	3.28	152.55
Kalra (2005)	R 106	0	23.30	406.63

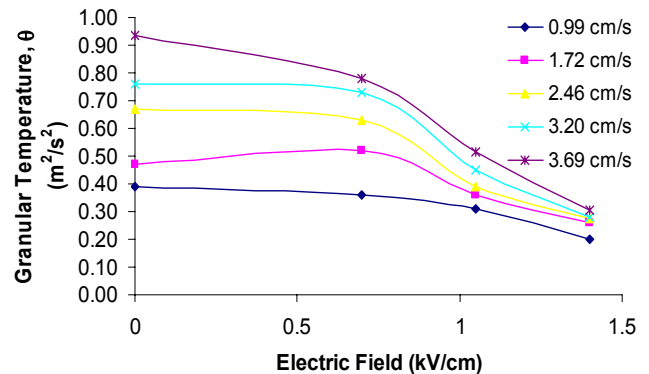


Figure 20. Effect of electric field on granular temperature, at various superficial gas velocities.

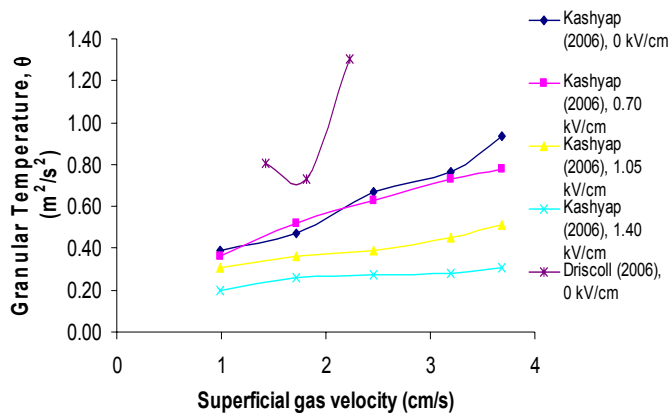


Figure 21. Effect of superficial gas velocity on granular temperature, at various electric fields.

Table 2. Dependence of granular temperature on superficial gas velocities and electric field strengths.

<u>Superficial</u> <u>gas velocity</u> <u>(cm/s)</u>	<u>Electric Field</u> <u>(kV/cm)</u>	<u>Granular</u> <u>Temperature, Θ</u> <u>(m^2/s^2)</u>
0.99	0	0.39
0.99	0.7	0.36
0.99	1.05	0.31
0.99	1.4	0.20
1.72	0	0.47
1.72	0.7	0.52
1.72	1.05	0.36
1.72	1.4	0.26
2.46	0	0.67
2.46	0.7	0.63
2.46	1.05	0.39
2.46	1.4	0.27
3.2	0	0.76

3.2	0.7	0.73
3.2	1.05	0.45
3.2	1.4	0.28
3.69	0	0.93
3.69	0.7	0.78
3.69	1.05	0.51
3.69	1.4	0.30